The stabilities, electronic structures and elastic properties of Rb–As systems

Havva Bogaz Ozisik[a)b)†], Kemal Colakoglu[a)], Engin Deligoz[b)], and Haci Ozisik[b)]

[a)] *Gazi University, Science Faculty, Physics Department,* 06500, *Teknikokullar, Ankara, Turkey*

[b)] *Aksaray University, Faculty of Arts and Science, Physics Department,* 68100, *Campus, Aksaray, Turkey*

(Received 29 September 2011; revised manuscript received 29 September 2011)

The structural, electronic and elastic properties of Rb–As systems (RbAs in NaP, LiAs and AuCu structures, $RbAs_2$ in the $MgCu_2$ structure, Rb_3As in Na_3As, Cu_3P and Li_3Bi structures, and Rb_5As_4 in the A_5B_4 structure) are investigated with the generalized gradient approximation in the frame of density functional theory. The lattice parameters, cohesive energies, formation energies, bulk moduli and the first derivatives of the bulk moduli (to fit Murnaghan's equation of state) of the considered structures are calculated and reasonable agreement is obtained. In addition, the phase transition pressures are also predicted. The electronic band structures, the partial densities of states corresponding to the band structures and the charge density distributions are presented and analysed. The second-order elastic constants based on the stress-strain method and other related quantities such as Young's modulus, the shear modulus, Poisson's ratio, sound velocities, the Debye temperature and shear anisotropy factors are also estimated.

Keywords: *ab-initio* calculations, structural properties, electronic properties, elastic properties, Rb–As compounds

PACS: 71.20.–b, 71.15.Mb, 62.20.–x **DOI:** 10.1088/1674-1056/21/4/047101

1. Introduction

Alkali metal pnictides are members of the Zintl phase family, which has drawn the attention of scientists in inorganic research for many years.[1,2] These materials show different physical and chemical properties depending on structure and chemical composition.[2−4] For different stoichiometries and structures, they possess a band gap range from 0.1 eV up to 2.5 eV. This important property is used in thin film and photocathode applications.[5,6] Some alkali pnictides are also used in crystal growth techniques.[7−9]

There have been many studies on alkali pnictides, but most of them are concerned with the compounds of the alkali metals with Sb and Bi elements. It has been reported recently that there are only a few theoretical or experimental studies on Rb–As compounds.[1,10−16] Therefore, we believe that more theoretical and experimental research efforts are needed to explore the various physical properties in different crystal structures and different stoichiometries of RbAs compounds. Sangster *et al.*[10] reported on the structural parameters and phase diagrams of the many compounds, including the Rb–As compounds in the NaP, Na_3As, Rb_4P_6, βRb_3P_7 and αNa_3P_{11} structures. Emmerling *et al.*[11] synthesized monoclinic Rb_3As_7 and orthorhombic RbAs compounds and characterized them via single crystal X-ray studies and Raman spectroscopy. Gnutzmann *et al.*[12] investigated the structural parameters of Rb_3As in Na_3As structures by X-ray powder diffraction. The crystal structure and bonding properties of orthorhombic Rb_4As_6 were determined by Hoenle *et al.*[13] Honle *et al.*[14] investigated the crystal structure of the low temperature modification of orthorhombic Rb_3As_7. Emmerling[15] characterized the crystal structure of Rb_3As_{11} in the Na_3P_{11} structure via single crystal X-ray studies. Theoretically, Xu and Jin[1] studied the geometrical structures, the electronic structures and the vibrational frequencies of $RbAs_5$ clusters with density functional theory. The bond lengths, atomization energies and vertical ionization potentials of RbAs and $RbAs_2$ clusters were determined by Igell-Mann and Stoll.[16]

To our knowledge, despite these efforts, information about the structural phase transitions, the electronic properties and the elastic properties, which are the important bulk properties, are not available for Rb–As compounds. Here, we aim to complete this lack of information by investigating the structural, electronic and elastic properties of Rb–As compounds for different stoichiometries and structures (RbAs in NaP, LiAs and AuCu structures, $RbAs_2$ in the $MgCu_2$

†Corresponding author. E-mail: havva.bogaz@gazi.edu.tr

© 2012 Chinese Physical Society and IOP Publishing Ltd

structure, Rb_3As in Na_3As, Cu_3P and Li_3Bi structures, and Rb_5As_4 in the A_5B_4 structure) in detail and interpret the salient results. Detailed crystallographic parameters of the considered structures are given in Table 1. The layout of this paper is as follows. The calculation method is given in Section 2, and the results and overall conclusion are presented and discussed in Sections 3 and 4, respectively.

Table 1. Crystallographic data for the considered structures of Rb–As compounds and the calculated atomic positions after local optimizations at the *ab initio* level (GGA-PBE).

Compound	Space group (number)	Structure	Atom	Site	GGA–PBE (present)	k-grid mesh
RbAs	$P2_12_12_1$ (19)	NaP	Rb_1	$4a$ (x_1, y_1, z_1)	$4a$ (0.3943, 0.9173, 0.0380)	$8 \times 8 \times 5$
	orthorhombic		Rb_2	4a (x_2, y_2, z_2)	$4a$ (0.1410, 0.6509, 0.3321)	
			As_1	$4a$ (x_3, y_3, z_3)	$4a$ (0.3245, 0.1595, 0.2813)	
			As_2	$4a$ (x_4, y_4, z_4)	$4a$ (0.4346, 0.4186, 0.1442)	
RbAs	$P2_1$/c (14)	LiAs	Rb_1	$4e$ (x_1, y_1, z_1)	$4e$ (0.2023, 0.3992, 0.3318)	$8 \times 8 \times 5$
	monoclinic		Rb_2	$4e$ (x_2, y_2, z_2)	$4e$ (0.2541, 0.6673, 0.0305)	
			As_1	$4e$ (x_3, y_3, z_3)	$4e$ (0.3434, 0.9049, 0.2788)	
			As_2	$4e$ (x_4, y_4, z_4)	$4e$ (0.3579, 0.1685, 0.1426)	
RbAs	$P4/mmm$ (123)	AuCu	Rb	$1a$ $(0, 0, 0)$	$1a$ $(0, 0, 0)$	$8 \times 8 \times 11$
	tetragonal		As	$1d$ $(1/2, 1/2, 1/2)$	$1d$ $(0.5, 0.5, 0.5)$	
$RbAs_2$	Fd-$3m$ (227)	$MgCu_2$	Rb	$8a$ $(1/8, 1/8, 1/8)$	$8a$ $(0.125, 0.125, 0.125)$	$6 \times 6 \times 6$
	cubic		As	$16d$ $(1/2, 1/2, 1/2)$	$16d$ $(0.5, 0.5, 0.5)$	
Rb_3As	$P6_3/mmc$ (194)	Na_3As	Rb_1	$2b$ $(0, 0, 1/4)$	$2b$ $(0, 0, 0.25)$	$10 \times 10 \times 6$
	hexagonal		Rb_2	$4f$ $(1/3, 2/3, 1/4)$	$4f$ $(0.3333, 0.6667, 0.5784)$	
			As	$2c$ $(1/3, 2/3, 1/4)$	$2c$ $(0.3333, 0.6667, 0.25)$	
Rb_3As	Fm-$3m$ (225)	Li_3Bi	Rb1	$4b$ $(1/2, 1/2, 1/2)$	$4b$ $(0.5, 0.5, 0.5)$	$7 \times 7 \times 7$
	cubic		Rb2	$8c$ $(1/4, 1/4, 1/4)$	8c (0.25, 0.25, 0.25)	
			As	$4a$ $(0, 0, 0)$	$4a$ $(0, 0, 0)$	
Rb_3As	$P6_3cm$ (185)	Cu_3P	Rb_1	$2a$ $(0, 0, z_1)$	$2a$ $(0, 0, 0.3020)$	$6 \times 6 \times 6$
	hexagonal		Rb_2	$4b$ $(1/3, 2/3, z_2)$	$4b$ $(0.3333, 0.6667, 0.2149)$	
			Rb_3	$6c$ $(x_1, 0, z_3)$	$6c$ $(0.2914, 0, 0.5766)$	
			Rb_4	$6c$ $(x_2, 0, z_4)$	$6c$ $(0.3705, 0, 0.9160)$	
			As	$6c$ $(x_3, 0, z_5)$	$6c$ $(0.3284, 0, 0.2455)$	
Rb_5As_4	$C2/m$ (12)	A_5B_4	Rb_1	$4i$ $(x_1, 0, z_1)$	$4i$ $(0.1097, 0, 0.4014)$	$6 \times 6 \times 6$
	monoclinic		Rb_2	$4i$ $(x_2, 0, z_2)$	$4i$ $(0.7552, 0, 0.1716)$	
			Rb_3	$2a$ $(0, 0, 0)$	$2a$ $(0, 0, 0)$	
			As_1	$4i$ $(x_3, 0, z_3)$	$4i$ $(0.4567, 0, 0.1961)$	
			As_2	$4i$ $(x_4, 0, z_4)$	$4i$ $(0.4082, 0, 0.3950)$	

2. Method of calculation

In the present paper, all calculations are carried out using the Vienna *ab initio* simulation package (VASP)[17–20] based on density functional theory (DFT). For the exchange and correlation terms in the electron–electron interaction, the Perdew–Burke–Ernzerhof (PBE) model[21] was used within the generalized gradient approximation (GGA). The electron–ion interaction was considered in the form of the projector-augmented-wave (PAW) method[18,22] with plane wave up to an energy of 450 eV. The k-mesh values determined by choosing k-point separation 0.02 $Å^{-1}$ (1 Å=0.1 nm) are given in Table 1, and they were found to be sufficient for the total energy calculations. Structural optimization was performed for each structure for all lattice constants, angles and internal atomic coordinates until the differences in total energy and maximum force were within 1.0×10^{-6} eV and 1.0×10^{-4} eV/Å, respectively. Structural optimization was performed for each structure for all lattice constants, angles and internal atomic coordinates. For a given volume of the unit cell, the lattice parameters are determined by minimizing the total energy. The data of total energy versus volume were fitted using Murnaghan's equation of state (EOS).[23] Besides the equilibrium volume, this fitting procedure gives the minimum value of the total energy E, the isothermal bulk modulus B, and its pressure derivative B' in the equilibrium state.

3. Results and discussion

3.1. Structural and electronic properties

We optimized the volume of the cell and the ionic positions of the atoms to obtain a relaxed structure. The obtained parameters were used to calculate other physical properties. The calculated atomic positions and lattice parameters are listed in Tables 1 and 2, along with those from the other available studies for comparison. The crystal structure models of the Rb–As systems in the NaP, LiAs, AuCu, Na_3As, Li_3Bi, Cu_3P and A_5B_4 structures are illustrated in Fig. 1.

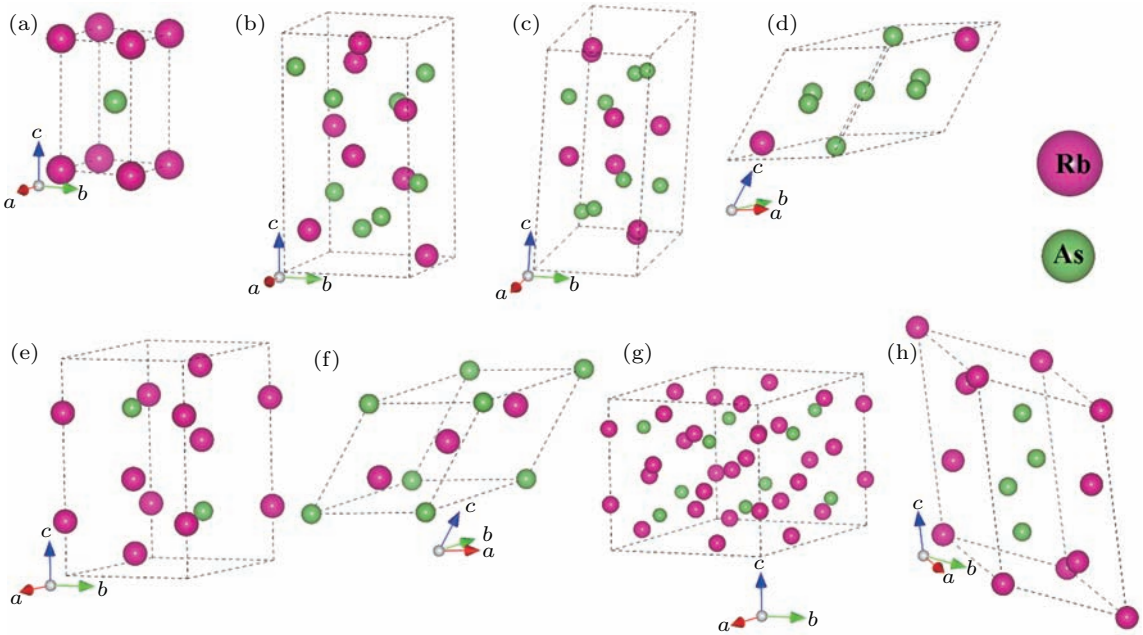


Fig. 1. (colour online) The crystal structure models of Rb–As compounds in (a) AuCu, (b) NaP, (c) LiAs, (d) Na_3As, (e) Li_3Bi, (f) Cu_3P and (g) A_5B_4 structures.

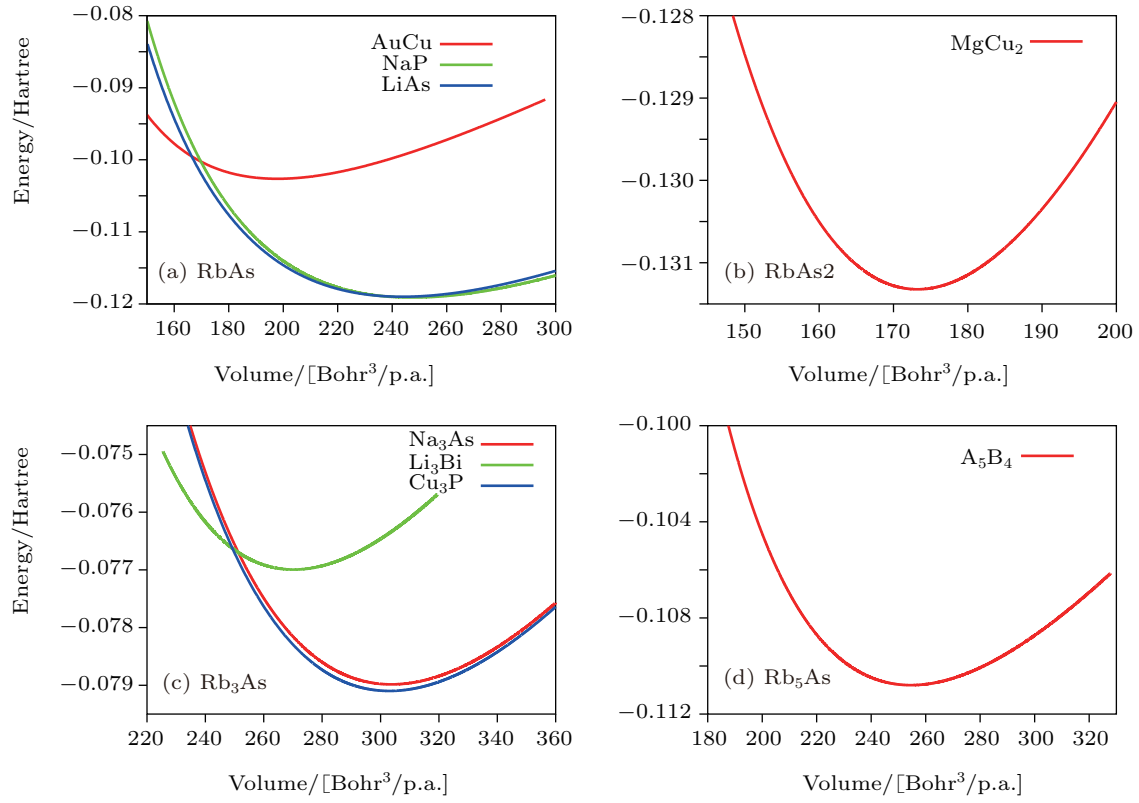


Fig. 2. (colour online) Energy–volume curves of the considered phases of the Rb–As compounds (1 Hartree=27.21 eV).

The crystal total energies are calculated for different values of lattice constants and fitted in terms of Murnaghan's EOS[23] (See Fig. 2). Their bulk moduli and pressure derivatives are also calculated based on the same Murnaghan's EOS, and the results are listed in Table 2. It can be seen that the present lattice parameters are in good agreement (around 2.5%) with the experimental results, except for the lattice constant (a) in Ref. [11].

As a fundamental physical property, the bulk modulus of the solid provides valuable information, including the average bond strengths of the atoms for the given crystals.[24] In the present case, the largest value of bulk modulus (41.4 GPa) is obtained for the $MgCu_2$ structure, and this implies that this structure is the least compressible among the others.

The cohesive energy is known as a measure of the strength of force, which binds atoms together in the solid state. In this context, the cohesive energies of Rb–As compounds are calculated in the considered structures. The values of cohesive energy ($E_{\rm coh}$) of the given structures are defined as

$$E_{\rm coh}^{{\rm Rb}_x{\rm As}_y} = E_{\rm total}^{{\rm Rb}_x{\rm As}_y} - \left[xE_{\rm atom}^{\rm Rb} + yE_{\rm atom}^{\rm As}\right], \qquad (1)$$

where $E_{\rm total}^{{\rm Rb}_x{\rm As}_y}$ is the total energy (in formula units) of the compound at equilibrium lattice constant, and $E_{\rm atom}^{\rm Rb}$ and $E_{\rm atom}^{\rm As}$ are the atomic energies of the pure constituents calculated with a large cutoff $r_{\max} = 15$ Å (free atom). Also, from the total energy of the compound and the constituent elemental solids (bcc W-type (Im-3m, #229, A2) for rubidium and rhombohedral α-As-type (R-3m, #166, A7) for the arsenic element), one can obtain the formation energy using the relation

$$E_{\rm form}^{{\rm Rb}_x{\rm As}_y} = E_{\rm total}^{{\rm Rb}_x{\rm As}_y} - \left[xE_{\rm solid}^{\rm Rb} + yE_{\rm solid}^{\rm As}\right]. \qquad (2)$$

The calculated cohesive and formation energies are listed in Table 2. These results imply that the present compounds possess negative formation energies and can easily be synthesized in various stable phases. The ranking orders of cohesive energy and formation energy are almost the same. The formation and cohesive energies of the NaP, $MgCu_2$, Cu_3P and A_5B_4 structures are higher than those of the other types of stoichiometry. It is seen from Table 2 that NaP and LiAs have almost the same formation energy, and the cohesive energy value also follows a similar trend.

The phase transition pressures of the Rb–As compounds are calculated from the Gibbs free energy at 0 K. The value of phase transition pressure is obtained from the same EOS data; phase transition occurs where the enthalpy difference between the two phases becomes zero (see Figs. 3 and 4). The phase transition pressure from the NaP (LiAs) to AuCu structure is found to be 12.7 (13.7) GPa with a 17.4% (16.2%) volume collapse. Also, the phase transition pressure from the Cu_3P (Na_3As) to Li_3Bi structure is calculated to be 2.1 (2.0 GPa) with a 10.0% (10.0%) volume collapse.

We also calculated the band structures of Rb–As compounds along the high symmetry directions using the calculated equilibrium lattice parameters. To the best of our knowledge, no experimental and theoretical data seem to be available to compare with our calculated results. It can be seen from Fig. 5 that 0.586 eV and 0.716 eV direct band gaps exist at Γ points for the NaP and LiAs structures, respectively, and a 0.220 eV indirect band gap exists from X to Γ for the Li_3Bi structure. The NaP, LiAs and Li_3Bi structures exhibit semiconductor characteristics, and the AuCu, $MgCu_2$, Na_3As, Cu_3P and A_5B_4 structures exhibit metallic characteristics.

Table 2. Calculated values of equilibrium lattice parameters (a, b and c in Å), bulk modulus (B in GPa), pressure derivatives (B'), band gap ($E_{\rm g}$ in eV), cohesive energy ($E_{\rm coh}$ in eV/f.u.) and formation enthalpy ($\Delta H_{\rm f}$ in eV/f.u.).

Compound	Structure	a	b	c	$B_{\rm eos}$	B'	$E_{\rm g}$	$E_{\rm coh}$	$\Delta H_{\rm f}$	Ref.
RbAs	NaP	7.0872	6.7340	12.2771	22.3	4.301	0.586	−6.483	−0.897	present
		6.915	6.575	12.040						Exp.[a]
		6.581	6.916	12.047						Exp.[b]
RbAs	LiAs	7.0828	6.7086	13.1949	23.0	4.178	0.716	−6.476	−0.891	present
RbAs	AuCu	4.6257		5.4414	26.3	4.452		−5.600	−0.014	present
$RbAs_2$	$MgCu_2$	8.5081			41.4	4.316		−10.721	−0.481	present
Rb_3As	Na_3As	6.1619		10.8856	10.6	4.168		−8.598	−1.149	present
		6.052		10.73						Exp.[c]
Rb_3As	Li_3Bi	8.6154			11.5	4.544	0.220	−8.381	−0.932	present
Rb_3As	Cu_3P	10.6759		10.8984	10.7	4.236		−8.610	−1.161	present
Rb_5As_4	A_5B_4	12.3837	5.4720	10.8647	20.0	4.408		−27.135	−3.861	present

[a] From Ref. [10], [b] From Ref. [11], [c] From Ref. [12].

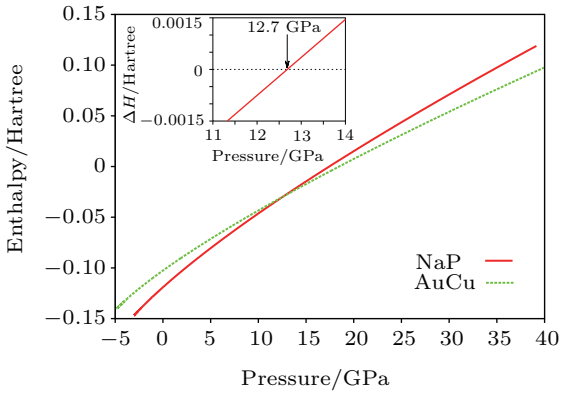


Fig.3. (colour online) Estimation of phase transition pressure from the NaP to AuCu structure for the RbAs compound (the same method is used for the other transitions).

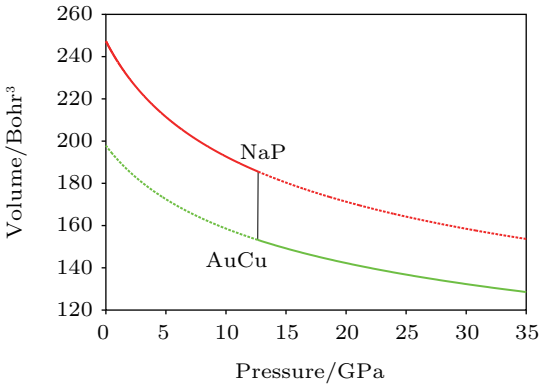


Fig.4. (colour online) Volume versus pressure curves of the RbAs compound in the NaP and AuCu structures (the same method is used for the other transitions).

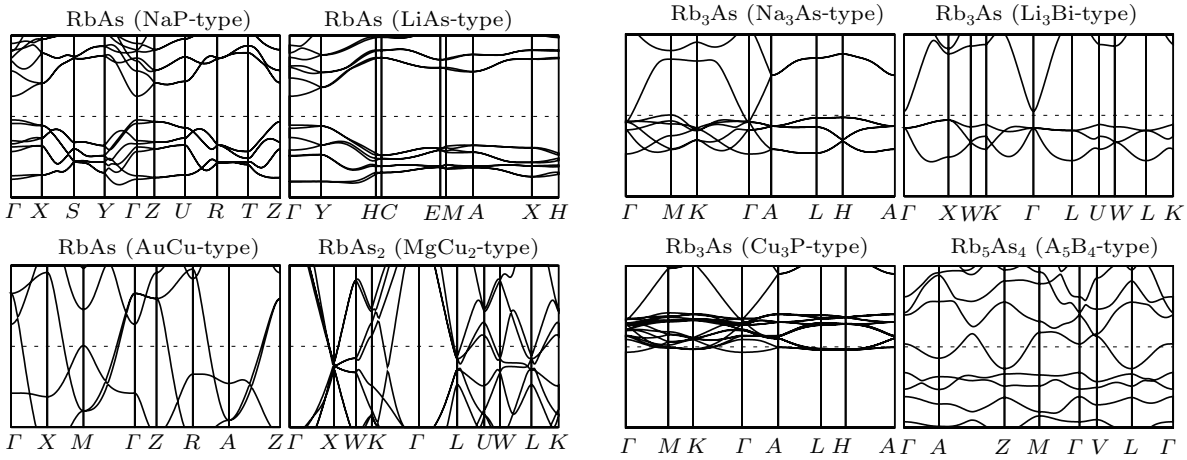


Fig. 5. The calculated band structures of the Rb–As compounds along high symmetry directions (the vertical axis represents energy ranging from −2 eV to 2 eV). The Fermi level is located at 0 eV.

The partial densities of states (PDOSs) corresponding to the band structures shown in Fig. 5 are also calculated and the obtained results are indicated in Figs. 6, 7 and 8. In Fig. 6, for the NaP structure the lowest valence bands occur at about −8.5 eV and −7.5 eV and are essentially dominated by As-s states. The other valence bands are dominated by As-p states, with a minor presence from other energetically degenerate states. The conduction band edge consists essentially of As-p states. Rb-d and As-p states dominate and energetically degenerate above 3 eV. The LiAs structure is similar to the NaP structure. The lowest valence bands occur above −8.5 eV and are essentially dominated by As-s states for the AuCu structure. The other valence bands are essentially dominated by As-p states. As-p states occur in the conduction band essentially dominated up to 3 eV, and then Rb-d states dominate.

In Fig. 7, the lowest valence bands occur at about −8.2 eV and are essentially dominated by As-s states for all compounds. The overall appearances of these compounds resemble each other. The other valence bands are essentially dominated by As-p states and the conduction bands are dominated by Rb-d states. These results indicate the existence of charge transfer and hence ionic character.

As seen from Fig. 8, the lowest valence band occurs at about −8.8 eV and is dominated by the As-s state in the $MgCu_2$ structure. The other valence bands and conduction bands are dominated by As-p states. For A_5B_4, the As-s states form higher peaks around −8.2 eV and −9.2 eV than the As-p states. The conduction bands between 0 and 1.4 eV are dominated by As-p states. Above 1.4 eV, Rb-d and As-p states dominate and show p-d hybridization.

To visualize the nature of the bonding characteristics in Rb–As compounds, we obtain the charge–density distributions for the NaP, LiAs, AuCu, $MgCu_2$, Na_3As, Li_3Bi, Cu_3P and A_5B_4 structures in the (−1 1 0), (−1 1 0), (1 1 0), (−1 1 0), (1 1 0), (−1 1 0), (1 0 0) and (−1 1 0) planes in Fig. 9, respectively. It can be seen that electronic distribution is high near the atomic cores. It is obviously shown that weak covalent bonding exists between the As atoms

and strong bonding occurs between the Rb and As atoms.

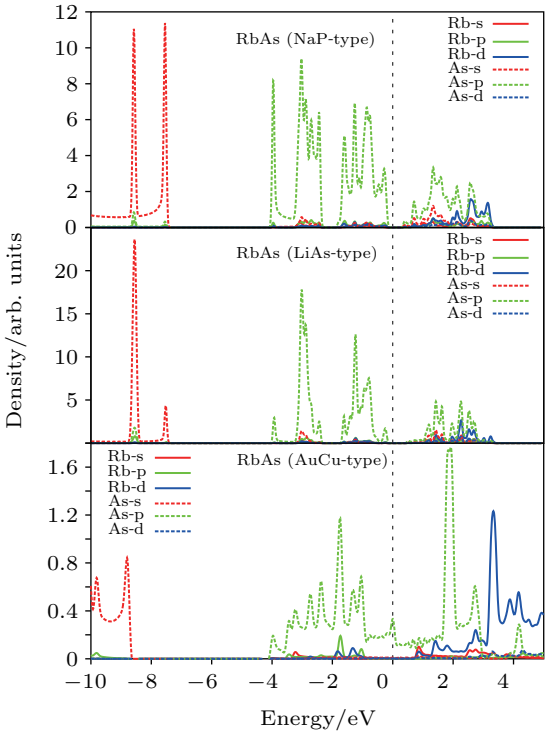


Fig. 6. (colour online) The calculated partial density of states of RbAs in NaP, LiAs and AuCu structures (the vertical axis is density (states/eV) in arbitrary units). The Fermi level is located at 0 eV.

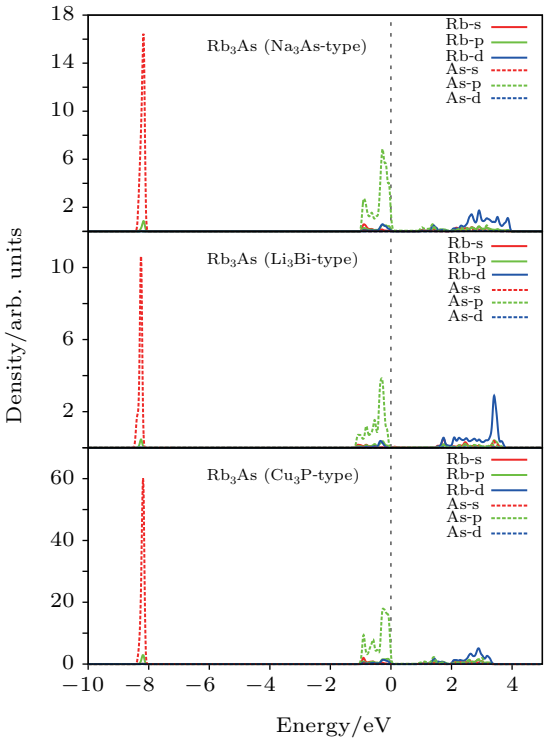


Fig. 7. (colour online) The calculated partial density of states of Rb_3As in Na_3As, Li_3Bi and Cu_3P structures (the vertical axis is density (states/eV) in arbitrary units). The Fermi level is located at 0 eV.

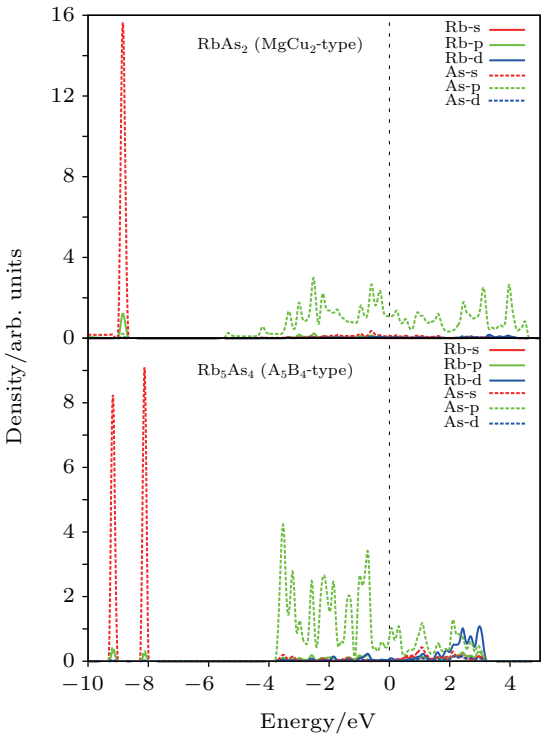


Fig. 8. (colour online) The calculated partial density of states of $RbAs_2$ and Rb_5As_4 in $MgCu_2$ and A_5B_4 structures, respectively (the vertical axis is density (states/eV) in arbitrary units). The Fermi level is located at 0 eV.

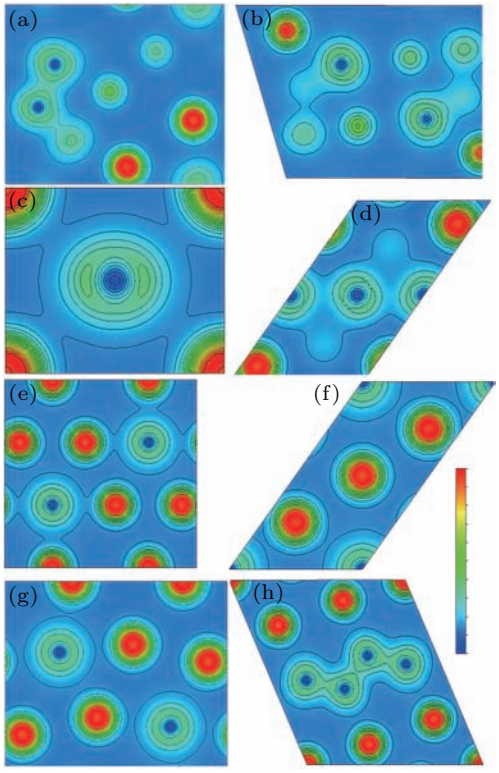


Fig. 9. (colour online) Electronic charge–density distributions for (a) NaP, (b) LiAs, (c) AuCu, (d) $MgCu_2$, (e) Na_3As, (f) Li_3Bi, (g) Cu_3P and (h) A_5B_4 structure in the (−110), (−110), (110), (−110), (110), (−110), (100) and (−110) planes, respectively.

3.2. Elastic properties

The elastic constant of a solid provides a link between the mechanical and dynamical behaviours of crystal, and gives important information concerning the nature of the force appearing in the solid. In particular, it provides information about the stability and stiffness of material, and its *ab initio* calculation requires an accurate method. Since the force and the elastic constant are functions of the first-order and the second-order derivatives of the potential, their calculations will provide a further check on the accuracy of the calculation of force in solids. The elastic constants are computed by using the "stress–strain" method,[25] and are listed in Table 3. For lattice stability, Born's stability criterion should be satisfied. Single crystalline elastic moduli and mechanical stability criteria for the considered structures can be found in Refs. [26] and [27].

Table 3. Calculated elastic constants (in GPa) of the Rb–As compounds in the considered structures.

Compound	Structure	C_{11}	C_{12}	C_{13}	C_{15}	C_{22}	C_{23}	C_{25}	C_{33}	C_{35}	C_{44}	C_{46}	C_{55}	C_{66}
RbAs	NaP	34.0	17.0	11.5		39.3	18.4		37.7		18.0		13.5	15.7
	LiAs	35.1	17.7	12.8	−5.1	39.9	18.0	−0.3	36.9	3.3	17.3	−0.3	14.5	16.5
	AuCu	46.9	8.8	12.6					86.9		24.9			−5.1
$RbAs_2$	$MgCu_2$	84.6	20.7								30.8			
Rb_3As	Na_3As	21.4	7.6	4.3					24.4		4.5			6.9
	Li_3Bi	13.9	10.5								11.7			
	Cu_3P	20.6	7.1	5.1					22.0		5.1			6.7
Rb_5As_4	A_5B_4	29.2	11.6	9.2	−0.8	32.8	7.6	0.6	63.7	4.9	12.2	0.8	11.9	12.2

It is known that the Voigt bound is obtained by the average polycrystalline moduli based on an assumption of uniform strain throughout a polycrystalline and is the upper limit of the actual effective modulus, while the Reuss bound is obtained by assuming a uniform stress and is the lower limit of the actual effective modulus.[27]

The bulk modulus (B), the shear modulus (G), Young's modulus (E) and Poisson's ratio (ν), which are the most interesting elastic properties for applications, are often measured for polycrystalline materials when investigating their hardnesses. We use the Hill average[28] to calculate Young's modulus (E) and Poisson's ratio (ν) by using the relations given in Refs. [29] and [30].

The calculated elastic constants are given in Table 3. Our results show that Rb–As compounds are mechanically stable at zero temperature and zero pressure, except for the AuCu structure. Several elastic constants are negative, but these negative values do not mean instability because the positive elastic coefficients can be yielded by the actually applied distortions.[31] The elastic constants C_{11}, C_{22} and C_{33} measure the a-, b- and c-direction resistances to linear compression, respectively. C_{33} is higher than C_{11} and C_{22} for the A_5B_4 structure and, similarly, C_{33} is higher than C_{11} for AuCu, so the c axis is less compressible than the other axes for these structures. It is known that the elastic constant C_{44} is the most important parameter indirectly governing the indentation hardness of a material. The calculated C_{44} for the $MgCu_2$ compound has the highest value. The large C_{44} means a strong ability to resist the monoclinic shear distortion in the (100) plane.

The calculated values of bulk modulus, isotropic shear modulus, Young's modulus and Poisson's ratio are given in Table 4. It is known that isotropic shear modulus and bulk modulus are a measure of the hardness of a solid. The bulk modulus is a measure of resistance to volume change by applied pressure, whereas the shear modulus is a measure of resistance to reversible deformations upon shear stress.[32] The calculated bulk modulus from the EOS and elastic constants are almost the same (see Tables 2 and 4). The shear modulus for the $MgCu_2$ structure is higher than the other ones.

Young's modulus is defined as the ratio of the tensile stress to the corresponding tensile strain, and it is a measure of the stiffness of the solid. The material is stiffer if the value of Young's modulus is high. Here, the highest value of Young's modulus (75.0 GPa) is found for the $MgCu_2$ structure, and it is stiffer than the other structures. According to Table 4, these compounds have almost soft characteristics.

The value of Poisson's ratio is indicative of the degree of directionality of the covalent bonds. The typical value of Poisson's ratio is about 0.1 for covalent materials and 0.25 for ionic materials.[33] The calculated Poisson's ratio is about 0.25, therefore ionic contributions in interatomic bonding are dominant for these compounds. Poisson's ratio also provides more information when dealing with the characteristics of the bonding forces than any other elastic constant. The lower and upper limits for central force solid are 0.25 and 0.5, respectively.[34] Inter-atomic forces are predominantly central forces for some structures (NaP, LiAs, Na_3As, Li_3Bi and Cu_3P) compared with the other ones ($MgCu_2$ and A_5B_4).

Table 4. Calculated values of bulk modulus (B), Young's modulus (E), shear modulus (G), Poisson's ratio (ν), Debye temperature ($\Theta_{\rm D}$), and sound velocities ($v_{\rm t}, v_{\rm l}, v_{\rm m}$) for the considered structures of the Rb–As compounds.

Compound	Structure	B	G	E	ν	B/G	$\Theta_{\rm D}$	$v_{\rm l}$	$v_{\rm t}$	$v_{\rm m}$
RbAs	NaP	22.5	13.3	33.3	0.2530	1.691	190	3327	1913	2124
	LiAs	23.0	13.1	33.0	0.2608	1.757	189	3313	1884	2095
$RbAs_2$	$MgCu_2$	42.0	31.2	75.0	0.2022	1.346	276	4059	2479	2738
Rb_3As	Na_3As	11.0	6.2	15.6	0.2627	1.774	132	2504	1420	1579
	Li_3Bi	11.6	5.5	14.2	0.2952	2.109	123	2345	1264	1411
	Cu_3P	10.8	6.3	15.8	0.2558	1.714	133	2502	1433	1592
Rb_5As_4	A_5B_4	19.5	13.0	31.9	0.2273	1.500	188	3221	1913	2118

According to the criterion,[35,36] a material is brittle (ductility) if the B/G ratio is less (high) than 1.75. Therefore, NaP, $MgCu_2$, Cu_3P and A_5B_4 are classified as being brittle, and the others (LiAs, Na_3As, Li_3Bi) are classified as being ductile in nature. Moreover, for covalent and ionic materials the typical relations between bulk and shear moduli are $G \approx 1.1B$ and $G \approx 0.8B$, respectively.[33] Here, the values of the G/B ratio for all compounds strongly support the ionic contribution to inter-atomic bonding.

The Debye temperature is known as an important fundamental parameter that is closely related to many physical properties such as specific heat and melting temperature. At low temperatures the vibrational excitations arise solely from acoustic vibrations. Hence, at low temperatures the Debye temperatures calculated from elastic constants are the same as those determined from specific heat measurements. We have calculated the Debye temperatures and sound velocities by using the common relation given in Refs. [37] and [38]. The calculated Debye temperatures are listed in Table 4 for the studied structures. The lowest Debye temperature value is that of the Li_3Bi structure. Generally, the Debye temperature for soft (hard) material is lower (higher).[39] These compounds possess low Debye temperatures, so again one concludes that these are the soft materials.

The anisotropies of crystals affect the physical properties in different directions of solids, e.g. cracks and dislocations can be induced by elastic anisotropy.[40] The shear anisotropic factors measure the degrees of anisotropy in the bonding between atoms in different planes. For an isotropic crystal, the values of A_1, A_2 and A_3 equal 1 and any value smaller or greater than 1 is a measure of the degree of shear anisotropy. The shear anisotropy factors are given as $A_1 = 4C_{44}/(C_{11} + C_{33} - 2C_{13})$ for the $\{100\}$ shear plane between $\langle 011\rangle$ and $\langle 010\rangle$ directions, $A_2 = 4C_{55}/(C_{22} + C_{33} - 2C_{23})$ for the $\{010\}$ shear plane between $\langle 101\rangle$ and $\langle 001\rangle$ directions, and similarly, $A_3 = 4C_{44}/(C_{11} + C_{22} - 2C_{12})$ for the $\{001\}$ shear plane between $\langle 110\rangle$ and $\langle 010\rangle$ directions. The shear anisotropy factors are given as $A_1 = A_2 = A_3$, and $A_1 = A_2$ for cubic and hexagonal structures, respectively. In addition, we also calculate the percentage elastic anisotropies for polycrystalline material, which are defined as $A_B = (B_{\rm V} - B_{\rm R})/(B_{\rm V} + B_{\rm R})$ and $A_G = (G_{\rm V} - G_{\rm R})/(G_{\rm V} + G_{\rm R})$ for compressibility and shear, respectively, where the subscripts V and R represent the Voigt and Reuss approximations, respectively. In these expressions, the zero value corresponds to the elastic isotropy and the value of 100% indicates the largest elastic anisotropy. Our results are listed in Table 5 for Rb–As compounds. $MgCu_2$ is elastically isotropic and has relatively low percentages of anisotropy in compression and shear. Na_3As and Cu_3P are elastically isotropic for the $\{001\}$ shear planes and elastically anisotropic for the $\{100\}$ ($\{010\}$) shear planes. A_5B_4 has an elastically anisotropic structure, and Li_3Bi possesses the highest anisotropy and percentage of anisotropy in shear among all the compounds.

Table 5. Calculated values of shear anisotropic factors (A_1, A_2 and A_3) and the percentage of anisotropy in compression and shear (A_B and A_G).

Compound	Structure	A_1	A_2	A_3	A_B/%	A_G/%
RbAs	NaP	1.478	1.343	1.598	0.972	2.897
	LiAs	1.487	1.416	1.671	0.829	5.958
$RbAs_2$	$MgCu_2$	0.964				
Rb_3As	Na_3As	0.484		1	−0.299	4.594
	Li_3Bi	6.882				38.739
	Cu_3P	0.630		0.993	−0.300	1.861
Rb_5As_4	A_5B_4	0.653	0.588	1.259	3.849	5.595

4. Conclusions

We calculated the structural, electronic and mechanical properties for Rb–As systems using the first-principles calculations based on the generalized gradient approximation (GGA) implemented using VASP. The calculated lattice parameters are in agreement with the available experimental values. The cohesive energies of Rb–As compounds are all negative, showing that they are thermodynamically stable. The phase transition pressure from the NaP (LiAs) to AuCu structure and from the Cu_3P (Na_3As) to Li_3Bi structure are found to be 12.7 (13.7) GPa and 2.1 (2.0) GPa, respectively. According to the band structure and DOS profiles, NaP, LiAs and Li_3Bi structures exhibit semiconductor characteristics and AuCu, $MgCu_2$, Na_3As, Cu_3P and A_5B_4 structures exhibit metallic characteristics. The bonding behaviour between the Rb atom and As atom in the Rb–As compound is a combination of covalent and ionic nature. Our results for elastic constants satisfy the traditional mechanical stability conditions for these compounds, except for RbAs in the AuCu structure. Also, the values of bulk modulus, shear modulus, Young modulus, Debye temperature and elastic wave velocity of Rb–As compounds in the considered structures are lower than those of the Na–As compounds in Ref. [41]. Moreover, NaP, $MgCu_2$, Cu_3P and A_5B_4 structures are classified as being brittle, and the other structures are classified as being ductile in nature. Consequently, we conclude that our theoretical predictions on the considered properties of these compounds could serve as a reliable reference for further experimental and theoretical investigations.

References

[1] Xu W G and Jin B 2006 *J. Mol. Struc. Theochem* **759** 101

[2] Burtzlaff S, Holynska M and Dehnen S 2010 *Z. Anorg. Allg. Chem.* **636** 1691

[3] Tegze M and Hafner J 1992 *J. Phys.*: *Condens. Matter* **4** 2449

[4] Derrien G, Tillard M, Manteghetti A and Belin C 2003 *Z. Anorg. Allg. Chem.* **629** 1601

[5] Ettema A R H F and de Groot R A 1999 *J. Phys.*: *Condens. Matter* **11** 759

[6] Hirt H and Deiseroth H 2004 *Z. Anorg. Allg. Chem.* **630** 1357

[7] Yan J Q, Nandi S, Zarestky J L, Tian W, Kreyssig A, Jensen B, Kracher A, Dennis K W, McQueeney R J, Goldman A I, McCallum R W and Lograsso T A 2009 *Appl. Phys. Lett.* **95** 222504

[8] Chen Z G, Yuan R H, Dong T and Wang N L 2010 *Phys. Rev.* B **81** 100502

[9] Dong T, Chen Z G, Yuan R H, Hu B F, Cheng B and Wang N L 2010 *Phys. Rev.* B **82** 054522

[10] Sangster J and Pelton A D 1993 *J. Phase Equilibria* **14** 243

[11] Emmerling F and Röhr C 2002 *Z. Naturforsch* B **57** 963

[12] Gnutzmann G, Dorn F W and Klemm W 1961 *Zeitschrift fuer Anorganische und Allgemeine Chemie* **309** 210

[13] Honle W, Krogull G, Peters K and Von Schering H G 1999 *Kristallogr.* **214** 17

[14] Honle W, Buresch J, Wolf J, Peters K, Chang J H and Von Schering H G 2002 *Z. Kristallogr.* **217** 489

[15] Emmerling F and Röhr C 2003 *Z. Anorg. Allg. Chem.* **629** 467

[16] Igel-Mann G and Stoll H 1994 *Compd. Mater. Sci.* **2** 413

[17] Kresse G and Hafner J 1994 *Phys. Rev.* B **47** 558

[18] Kresse G and Joubert D 1999 *Phys. Rev.* B **59** 1758

[19] Kresse G and Furthmuller J 1996 *Compd. Mater. Sci.* **6** 15

[20] Kresse G and Furthmuller J 1996 *Phys. Rev.* B **54** 11169

[21] Perdew J P, Burke K and Ernzerhof M 1996 *Phys. Rev. Lett.* **77** 3865

[22] Blochl P E 1994 *Phys. Rev.* B **50** 17953

[23] Murnaghan F D 1937 *Am. J. Math.* **49** 235

[24] Maradudin A A, Montroll E W, WeissG H and Ipatova I P 1971 *Theory of Lattice Dynamics in the Harmonic Approximation* 2nd edn. (New York, London: Academic Press)

[25] Page Y L and Saxe P 2001 *Phys. Rev.* B **63** 174103

[26] Ozisik H, Colakoglu K, Ozisik H B and Deligoz E 2011 *Compd. Mater. Sci.* **50** 349

[27] Wu Z, Zhao E, Xiang H, Hao X, Liu X and Meng J 2007 *Phys. Rev.* B **76** 054115

[28] Hill R 1952 *Proc. Phys. Soc. Lond.* **65** 349

[29] Voigt W 1928 *Lehrburch der Kristallphysik* (Leipzig: Teubner)

[30] Reuss A 1929 *Z. Angew. Math. Mech.* **9** 49

[31] Söderlind P and Klepeis J E 2009 *Phys. Rev.* B **79** 104110

[32] Florez M, Recio J M, Francisco E, Blanco M A and Penda's A M 2002 *Phys. Rev.* B **66** 144112

[33] Bannikov V V, Shein I R and Ivanovskii A L 2008 *Phys. Status Solidi* **R1** 89

[34] Fu H, Li D, Peng F, Gao T and Cheng X 2008 *Compd. Mater. Sci.* **44** 774

[35] Pugh S F 1954 *Philos. Mag.* **45** 823

[36] Shein I R and Ivanovskii A L 2008 *J. Phys.*: *Condens. Mater.* **20** 415218

[37] Johnston L, Keeler G, Rollins R and Spicklemire S 1996 *Solid State Physics Simulations, The Consortium for Upper-Level Physics Software* (New York: Jhon Wiley)

[38] Schreiber E, Anderson O L and Soga N 1973 *Elastic Constants and Their Measurements* (New York: McGraw-Hill)

[39] Zhao E, Wang J and Wu Z 2010 *J. Comput. Chem.* **31** 2883

[40] Miao N, Sa B, Zhou J and Sun Z 2011 *Compd. Mater. Sci.* **50** 1559

[41] Ozisik H B, Colakoglu K, Deligoz E and Ozisik H 2011 *Solid State Commun.* **151** 1349